JOURNAL OF AGRICULTURAL AND FOOD CHEMISTRY

Nondestructive Evaluation of Anthocyanins in Olive (*Olea europaea*) Fruits by in Situ Chlorophyll Fluorescence Spectroscopy

GIOVANNI AGATI,*,† PATRIZIA PINELLI,‡ SOLANGE CORTÉS EBNER,§ ANNALISA ROMANI,‡ AURÉLIE CARTELAT,|| AND ZORAN G. CEROVIC||

Istituto di Fisica Applicata 'Nello Carrara', CNR, Via Madonna del Piano (Edificio C), I-50019 Sesto Fiorentino, Italy, Dipartimento di Scienze Farmaceutiche, Università degli Studi di Firenze, Via U. Schiff 6, 50019 Sesto F.no (FI), Italy, Dipartimento di Scienze e Tecnologie Ambientali Forestali, Università degli Studi di Firenze, Via S. Bonaventura 11-13, 50145 Firenze, Italy, and Equipe Photosynthèse et Télédétection, LURE−CNRS, Bât 203, Centre Universitaire Paris-Sud, BP 34, F-91898 Orsay, France

Anthocyanins (Anths) in olive (*Olea europaea* L.) fruits at different degrees of pigmentation were assessed nondestructively by measuring chlorophyll fluorescence (ChlF). The method is based on the comparison of the ChlF excitation spectra from olives with different pigmentation from green to green−red, reddish−purple, and purple. The logarithm of the ratio between the fluorescence excitation spectra (logFER) from two different colored zones gave the difference in the absorption spectrum between them. The absorbance spectrum derived from the logFER between a red olive and the same olive devoid of the skin showed the typical Anth green band (at 550 nm). It matched that recorded by microspectrophotometry on a single pulp cell and the in vitro absorbance spectrum of the olive skin extract. As expected, the in vivo Anths absorption maximum increased in intensity going from less to more mature olives and was higher in the sun-exposed olive side with respect to the sun-shaded side. Absolute quantitative nondestructive determination of Anths for each olive sample was obtained by the logFER calculated for two excitation wavelengths, 550 and 625 nm, of ChlF at 740 nm. Going from green to purple skin colors, the Log[ChlF(625)/ChlF(550)] was fairly well-correlated to the extract Anths concentration. Finally, the relationship between the Anths and the other main phenolics present in the olives analyzed by high-performance liquid chromatography was evaluated. The main result was a net increase of verbascoside with increasing Anths content. On the basis of our results, the development of a new rapid and noninvasive method for the monitoring of olive development and ripening can be envisaged.

KEYWORDS: Anthocyanins; chlorophyll fluorescence; *Olea europaea*; olive; ripening; fluorescence excitation spectra; polyphenols

INTRODUCTION

Olea europaea L., a member of the Oleaceae family, is probably the most ancient cultivated species in the world (*1*, *2*) and possesses an important economical impact for the production of olive oil. The quality of virgin olive oil is largely dependent on the amount and the composition of phenolic compounds of fruits at harvesting. These compounds determine oil taste and stability against oxidation (*3*), as well as the oil nutritional (*4*) and therapeutic characteristics (*5*). More hydrophilic compounds, such as verbascoside, that cannot be found in the oil but are present in olive oil industry wastewaters (*6*), are still of interest from a pharmacological point of view because of their peculiar antioxidant properties. Hence, there is much interest in developing agronomic techniques that maximize particular classes of olive phenolics. Several factors affect the phenolic composition and quantity in olive fruits, such as cultivar, growing site, climatic conditions, alternate bearing, and ripening stage. Because of this plurality of factors, finding a general objective criterion to establish the best harvest time related to the highest quality of olive oil is a difficult task.

A widely accepted practice is to use the maturation index suggested two decades ago by the International Olive Oil Council (*7*) derived from the visual classification of the skin

* To whom correspondence should be addressed. Tel: +39 055 5225 306. Fax: +39 055 5225 305. E-mail: G.Agati@ifac.cnr.it.
† Istituto di Fisica Applicata 'Nello Carrara'.
‡ Dipartimento di Scienze Farmaceutiche, Università degli Studi di Firenze.
§ Dipartimento di Scienze e Tecnologie Ambientali Forestali, Università degli Studi di Firenze.
|| LURE−CNRS.

10.1021/jf048381d CCC: $30.25
Published on Web 02/10/2005

color of olives (*8*). Indeed, fruit ripening is accompanied by a change in the skin color due to a modification of pigment concentration in the superficial tissues. Usually, color development from green to purple is modulated by an accumulation of anthocyanins (Anths) (*9*) together with the degradation of chlorophylls (Chls) and carotenoids (*10*). This feature suggests the use of optical methods to follow the maturation process, as applied to other kinds of fruits (*11*). Spectroscopic techniques can assess rapidly and nondestructively both photosynthetic and accessory pigments in fruits, more advantageously than standard, time-consuming extraction procedures. The drawback of noninvasive optical methods is that only superficial layers can be analyzed due to the limited penetration of radiation inside the sample. However, spectral signatures of fruit peculiarities localized inside the pulp, which are correlated to a surface-related compound, can still be obtained.

Anths are suitable for in situ spectroscopic detection since they accumulate in the outer layers of olives and present a characteristic absorption band in the green region around 530 nm. Because Anths are synthesized through the phenylpropanoid pathway, it is expected that their increase in concentration during ripening be correlated to a change in the content of other phenolic compounds. Such a relationship was proven for Anths and flavonols during the ripening of bilberries (*12*). In olives, previous studies have reported a general decrease of total phenolics as maturation proceeds, while specific compounds may have different trends during ripening (*13*−*15*). Metabolic links between oleuropein, verbascoside, and caffeic acid during ripening have been suggested (*13*, *16*); however, a direct quantitative relationship between Anths and other phenolic compounds is still lacking. Although several reports on phenolic compounds in olives have been published (*9*), only few data about Anths in *O. europaea* fruits are available (*17*−*19*).

Recently, methods using chlorophyll fluorescence (ChlF) to assess in situ the UV-absorbing phenolics in the leaf epidermis have been developed (*20*−*22*). These methods are based on the Chl fluorescence excitation ratio (FER), that is, the ratio of ChlF intensities under UV and blue−green excitation (*20*), UV and green excitation (*21*), or two whole ChlF excitation spectra (*22*). The fluorescence intensity emitted by the chloroplasts in the mesophyll is dependent on the amount of light reaching them. Because the UV radiation is much more attenuated with respect to visible light in the epidermal layers, comparing the ChlF induced by two different wavelengths, visible and UV, can provide information on the superficial concentration of the UV-absorbing compounds. The logarithm of the FER (logFER) was proven to be a quantitative measure of epidermal absorbance (*21*). On the basis of the logFER method, a portable leaf-clip device has been developed (*23*) and tested successfully in field measurements on wheat (*24*). Another type of device also based on double excitation but using fiber optics has recently been announced (*25*). This device, named UV-A PAM, has been used on fruits (grapevine berries) in addition to leaves (*26*).

By measuring entire ChlF excitation spectra instead of only two excitation bands, the whole absorption spectrum of leaf epidermis could be obtained (*22*). This is useful when both UV absorbers and visible pigments are present in the epidermis and permit their identification.

In the present study, we applied the ChlF excitation method to nondestructively assess the Anth content in olives with different skin pigmentation, corresponding to different maturation levels. We found that the logFER approach is suitable to detect the in vivo Anth absorption spectrum. Furthermore, the deduced Anth absorbances were nicely correlated, going from green to purple skin colors, to those measured spectrophotometrically in vitro after ethanol/water extraction of the very same olive area used for the ChlF measurements. In addition, we analyzed the phenolic composition of single olive samples in order to evaluate a possible correlation between specific phenolic compounds and Anths during fruit ripening.

Figure 1. Olives from the Frantoio cultivar at different pigmentation stages: green (I), green–red (II), red (III), red–purple (IV), and purple (V).

MATERIALS AND METHODS

Samples. Olives used in our study came from three different early ripening Tuscany cultivars of *O. europaea* L.: Frantoio, Leccino, and Moraiolo. Fruits with the widest range of skin colors were picked by hand at the end of September 2003 from trees of an established grove in Pieve a Celle, Pistoia, Italy (43° 55′ N, 10° 51′ E). They were classified according to five different color levels: green (I), green−red (II), red (III), reddish−purple (IV), and purple (V), as shown in **Figure 1** for the Frantoio cultivar.

Fluorescence Measurements. Excitation and emission fluorescence spectra of intact olives were acquired by a spectrofluorometer (Cary Eclipse, Varian, Les Ulis, France) through a double arm optical fiber bundle (C Technologies, Cedar Knolls, NJ) made of 147 randomized UV fibers. The two arms of the bundle were coupled to the excitation and emission parts of the spectrofluorometer via a fiber optic coupler accessory provided by Varian (part no. FA-VAR00-AP15). The common end of the fiber bundle was maintained at a fixed distance (5 mm) from the olive sample using a proprietary clip.

For each sample, excitation spectra were recorded in the 290−625 nm range for both the 685 and the 740 nm emission wavelengths. Emission spectra were measured between 645 and 845 nm with the excitation at 438 nm. Excitation and emission spectra were corrected using rodhamine B as a quantum counter and the quinine sulfate dihydrate standard with well-known traceable fluorescence emission properties, respectively. In addition, spectra were expressed in quinine sulfate equivalent units (QSEU) as previously suggested (*27*): 1000 QSEU corresponds to the fluorescence of 1 μM quinine sulfate dihydrate in 0.105 mol L^{-1} perchloric acid for 1 cm light path square cells or, in general, 1 nmol cm^{-2} for short light pass flat cells, excited at 347.5 nm and emitted at 450 nm under the identical conditions used to acquire the sample fluorescence spectrum. This normalization allows for quantitative comparison among fluorescence data measured on different samples, in different time periods, under different experimental conditions and different spectrofluorometers.

Fluorescence Excitation Spectra Elaboration. The theoretical basis for determining in vivo pigment absorbance in leaves from the ChlF measurements has previously been described (*21*, *22*). Briefly, pigments accumulated on the outer tissue layers attenuate the excitation light that can reach the chloroplasts. This filtering effect affects differently the various excitation wavelengths according to the absorbance spectral properties of the compounds. Therefore, for a given emission wavelength, for example, the red peak at 685 nm, the ChlF excitation spectrum can be expressed as:

$$\mathrm{Chl}F^{685}(\lambda_{ex}) = I(\lambda_{ex}) \cdot T(\lambda_{ex}) \cdot A_{Chl}(\lambda_{ex}) \cdot \Phi_f(\lambda_{ex}) \quad (1)$$

where I is the incident irradiance, T is the transmittance of the epidermal layers, A_{Chl} is the Chl absorption efficiency, and Φ_f is the ChlF apparent quantum yield. Comparing two samples with different epidermal pigment concentrations, s_1 and s_2, under identical irradiation and detection conditions, the ratio of the relative ChlF excitation spectra will be

$$\frac{\mathrm{Chl}F_{s_1}^{685}(\lambda_{ex})}{\mathrm{Chl}F_{s_2}^{685}(\lambda_{ex})} = \frac{I(\lambda_{ex}) \cdot T_{s_1}(\lambda_{ex}) \cdot A_{Chl}(\lambda_{ex}) \cdot \Phi_f(\lambda_{ex})}{I(\lambda_{ex}) \cdot T_{s_2}(\lambda_{ex}) \cdot A_{Chl}(\lambda_{ex}) \cdot \Phi_f(\lambda_{ex})} = \frac{T_{s_1}(\lambda_{ex})}{T_{s_2}(\lambda_{ex})} \quad (2)$$

According to the Beer−Lambert's law ($A = -\log T$), the logarithm of the ChlF ratio equals the difference in the epidermal absorbance between s_2 and s_1:

$$\log \frac{\mathrm{Chl}F_{s_1}^{685}(\lambda_{ex})}{\mathrm{Chl}F_{s_2}^{685}(\lambda_{ex})} = A_{s_2} - A_{s_1} \quad (3)$$

When the pigment of interest is absent in one of the samples, let us say s_1, A_{s_1} will be null and eq 3 will give the absorption spectrum of the s_2 (additional) compound.

Estimation of Anths by Dual Wavelength ChlF Excitation. Absolute quantitative nondestructive determination of Anths for each olive sample was obtained by the logFER calculated for two excitation wavelengths of ChlF. The theoretical basis for this has been reported by Ounis et al. (*21*). According to these authors, the FER for excitation wavelengths λ_1 and λ_2 and emission at 740 nm can be written

$$\frac{\mathrm{Chl}F^{740}(\lambda_1)}{\mathrm{Chl}F^{740}(\lambda_2)} = \frac{T(\lambda_1)}{T(\lambda_2)} + \frac{1 - 10^{-[\epsilon_a(\lambda_1)c_a + \epsilon_b(\lambda_1)c_b]l}}{1 - 10^{-[\epsilon_a(\lambda_2)c_a + \epsilon_b(\lambda_2)c_b]l}} \quad (4)$$

where ϵ_a, c_a and ϵ_b, c_b are the molar extinction coefficients and concentrations for Chl a and Chl b, respectively, and l is the optical path length inside the sample. We chose detection at the far-red band (740 nm) to avoid any Chl reabsorption effect.

The first term on the right side of eq 4 represents the ratio of the epidermal layer transmittances at the two excitation wavelengths. By choosing λ_1 inside the Anth absorption band and λ_2 (the reference) outside of it, therefore $T(\lambda_2) = 1$, the above FER relates directly to the Anth content. The last term in eq 4 contains an unwanted dependency on Chl a and Chl b concentrations. Because Chls are known to decrease during fruit ripening, this term may introduce a distortion factor in the relationship between FER and epidermal transmittance. However, this contribution can be removed or minimized by choosing two excitation wavelengths at which the Chl a and Chl b extinction coefficients are nearly equal. On the other hand, the distortion effect due to Chl changes is not expected to be important in thick samples, like fruits, where the optical path length, l, is large. A good compromise between the above conditions of choice of the excitation wavelengths was 550 and 625 nm, for λ_1 and λ_2, respectively, for which

$$\log \frac{\mathrm{Chl}F^{740}(625)}{\mathrm{Chl}F^{740}(550)} = A(550) + \log \frac{1 - 10^{-[\epsilon_a(625)c_a + \epsilon_b(625)c_b]l}}{1 - 10^{-[\epsilon_a(550)c_a + \epsilon_b(550)c_b]l}} \quad (5)$$

Using the in vitro (MeOH solution) Chl molar extinction coefficients (*27*) and Chl a and b concentrations measured in the sampled olives at different pigmentation stages, we found that the last term in eq 5 was not nil (about 0.5) but did not vary more than 7% with ripening. Curve fitting was performed by Table Curve 2D software (v3.04, Jandel Sci., CA) using the Simple Equations process.

Microspectrophotometry and Multispectral Microimaging. Hand-cut cross-sections (50−100 μm) of fresh olives mounted in water were immediately observed by the microscope system previously described (*28*). Absorbance spectra of olive pulp cells were obtained by measuring the light transmitted through the cross-section using a 40× objective lens and by comparing it to that transmitted from a zone just outside the sample. Spectra of transmitted light were recorded by a CCD (charge-coupled device) multichannel spectral analyzer (PMA 11-C5966, Hamamatsu, Photonics Italia, Arese, Italy) coupled to the microscope through an optical fiber bundle. Images were collected by a CCD camera (Chroma CX260, DTA, Italy) equipped with a motorized filter wheel carrying eight different interference filters. This detector permitted the sequential acquisition of transmittance and fluorescence images on specific spectral bands. Three transmittance images in the blue, green, and red regions, with integration times of 0.2 s, were sequentially acquired at 450, 550, and 680 nm, respectively. Monochrome images were then recombined in a single multicolor image using the RGB (red green blue) technique by the Image-Pro Plus v.4.0 software (Media Cybernetics, Silver Spring, MD). Fluorescence images of Chl were obtained by excitation at 365 nm (selected using a 10 nm bandwidth interference filter, 365FS10-25, Andover Corporation, Salem, NH), with a dichroic mirror at 400 nm (ND400, Nikon, Japan) and detection filter at 680 nm (10 nm bandwidth, 680FS10-25, Andover Corporation). Image spatial calibration using a 10× Plan Fluor (NA = 0.3) objective was 0.79 μm/pixel. Profiles of both ChlF (F^{680}) and transmittance at 550 nm (T^{550}) from the peel into the olive mesocarp were obtained by plotting the mean intensity of each longitudinal row of pixels vs the depth.

Olive Compound Extraction and Analysis. From each olive, immediately after the ChlF measurements, a disk (0.75 cm in diameter) from the sampled surface was extracted for 24 h with 2 mL of ethanol/water (70:30 v/v) acidified by HCl (pH 2.0). After the sample was filtered, absorbance spectra of extracts were measured by a diode array spectrophotometer (HP8453, Hewlett-Packard, Les Ulis, France). Anth content was determined as $A_{535} - A_{800}$ to remove a potential scattered light contribution. Correction for Chl absorbance overlapping as required in leaf extracts (*29*) was not needed since no significant amount of Chl was present in the olive disk extracts. Anth concentrations were expressed on an area basis using the extinction coefficient of 24.7 μmol^{-1} cm^2 (24.7 mM^{-1} cm^{-1}) at 532 nm, determined for a solution of a cyanidin-3-O-rutinoside standard in the same solvent.

Chl was extracted from separate samples, to avoid pheophytin formation, in pure MeOH at 70 °C for 30 min. Chl a and b concentrations were derived by absorbance measurements according to Lichtenthaler (*30*).

Extractions of phenolics from single destoned olive fruits of *O. europaea* L., cultivar Frantoio, were performed in 70% ethanol (pH 2.0) and then defatted with hexane. The alcoholic extract was concentrated under vacuum (Rotavapor 144 R, Büchi, Switzerland) and rinsed with 2 mL of a solution of MeOH/CH_3CN/H_2O, 60/20/20 (v/v/v), adjusted to pH 2.0 with formic acid. For each color level of the olive skin, three replicates were made. Quantitative analysis was performed using a HP-1100 liquid chromatograph equipped with a diode array detector (DAD) and a HP 1100 MSD API-electrospray (Agilent Technologies, Palo Alto, CA) operating in positive and negative ionization modes. Analytical conditions have previously been described (*18*). Identification of individual phenolics was carried out using their retention times and both spectroscopic and spectrometric data. Quantification of the single phenolic compound was directly performed by high-performance liquid chromatography (HPLC)-DAD using a four-point regression curve built with the available standards. Curves with a $r^2 > 0.9998$ were considered. Calibration was performed at the wavelength of maximum UV−vis absorbance applying the correction for molecular weight. In particular, hydroxytyrosol and its glucoside amounts were calculated at 280 nm using tyrosol as a reference; oleoside, demethyloleuropein, oleuropein, and its aglycone were calibrated at 280 nm using oleuropein as a reference; and verbascoside and hydroxyverbascoside were calculated at 330 nm using verbascoside as a reference compound. Finally, rutin and quercetin were calibrated at 350 nm using quercetin 3-O-rutinoside (rutin) as a reference. An HPLC-DAD analysis of olive fruit Anths was also carried out, following a previously reported method (*31*).

Oleuropein, tyrosol, and rutin were purchased from Extrasynthese S. A. (Lyon, Nord-Genay, France). All other reagents were of analytical grade and were purchased from Sigma (St. Louis, MO). All solvents were HPLC grade and were obtained from E. Merck (Darmstadt, Germany). Verbascoside was isolated by HPLC preparative chromatography as previously reported (*32*).

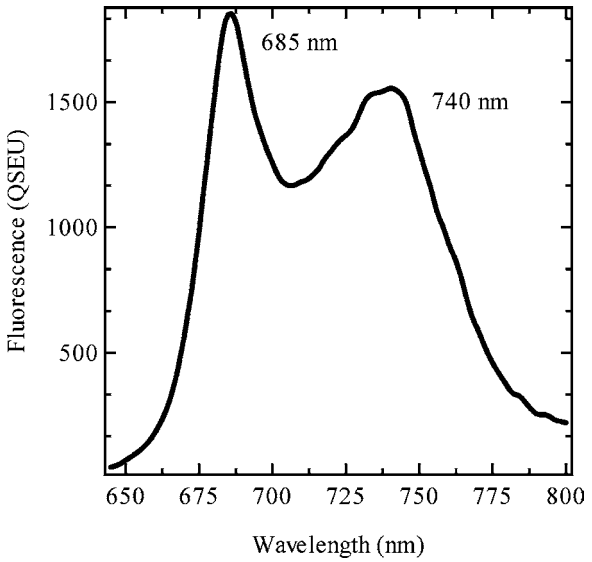

Figure 2. Fluorescence spectrum of a green olive (color level I, Frantoio) excited at 438 nm.

RESULTS AND DISCUSSION

Identification of Anths from ChlF Excitation Spectra. The emission spectrum recorded on the surface of an olive fruit was, as expected, similar to that observed in leaves, with two bands in the red, 685 nm, and the far-red, 740 nm, region (**Figure 2**). The spectral shape, that is, the red/far-red band ratio, depends on a reabsorption effect by Chl itself occurring at 685 nm (*33*, *34*). In fact, fluorescence emitted from chloroplasts inside the fruit tissues undergoes multiple scattering and absorption processes before emerging at the surface where it is detected. The partial overlapping of the Chl absorption band with the fluorescence band at 685 nm induces a modification of the ChlF spectrum. The effect is much more pronounced in thick vegetable tissues, such as fruit tissues, where the light internal path length is largely increased. The far-red band is not affected by reabsorption.

The excitation spectrum of ChlF in olives is also similar to that observed in leaves (*22*). It represents the convolution of absorption spectra of Chl and the accessory photosynthetic pigments (carotenoids) that transfer the absorbed energy to Chl. In addition, excitation spectra contain the negative contribution of pigments that attenuate the excitation light reaching the chloroplasts such as flavonoids and hydroxycinnamates in the UV and Anths in the green spectral regions. These features are shown in **Figure 3a** where the excitation spectra (emission at 685 nm) of a red olive (color level III) and the same olive devoid of the skin (i.e., pulp) are reported. The fluorescence intensity in the pulp is higher than that from the intact olive over the whole excitation spectrum. The maximal excitation occurs at about 440 and 480 nm, corresponding to the principal absorption peaks of Chls, a and b, and carotenoids. Nonphotosynthetic pigments accumulated in the external layers can be revealed by the logFER obtained from the ChlF excitation of the olive and that of the pulp (**Figure 3b**, solid line). It shows two absorption bands in the UV at about 350 nm corresponding to flavonoids and hydroxycinnamates and in the green at 550 nm due to Anths. The Anth band is quite similar to that measured by microspectrophotometry on a single mesocarp cell close to the epidermis (**Figure 3b**, dotted line). The wider band shape of the cell spectrum is due to the contribution of Chl and carotenoids as well as to scattered light. The logFER spectrum is also in good agreement with the absorption spectrum of an olive disk extract in ethanol/water (pH 2.0) (**Figure 3c**, solid line). Here, again, both the UV-absorbing phenolic and the Anth bands are present. The UVA absorption band is mainly due to verbascoside, caffeic acid derivatives, and flavonoids. The Anth band is shifted to shorter wavelengths (peak at 535 nm) with

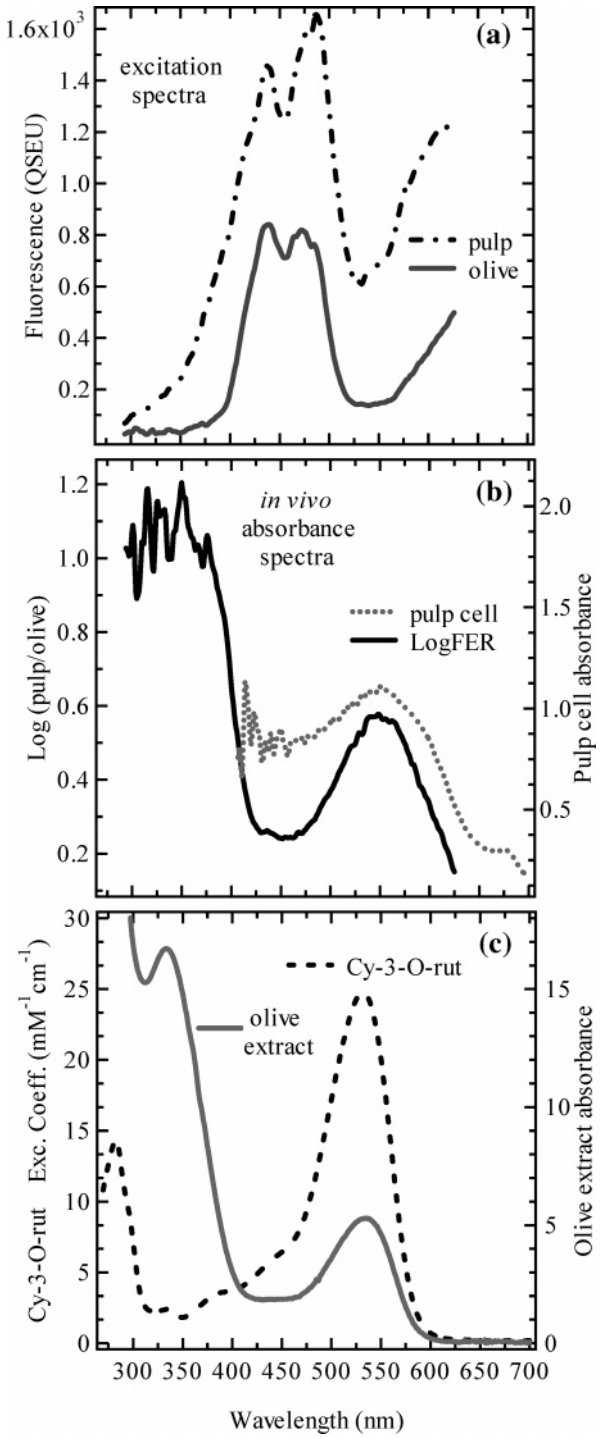

Figure 3. Fluorescence excitation and absorption spectra from olive, olive cell, and olive extract. (**a**) ChlF excitation spectra obtained from an olive (color level III) and the same olive devoid of the most outer layers (pulp); the emission wavelength was set at 685 nm. (**b**) Absorbance spectrum derived from the logFER between the olive pulp and the whole olive (solid line) as compared to the absorption spectrum measured on a pulp cell by microspectrophotometry on an olive cross-section. (**c**) Absorbance spectrum of a disk olive extract in ethanol/water (pH 2.0) (solid line) along with the extinction coefficient spectrum of cyanidin-3-O-rutinoside in the same solvent (dashed line).

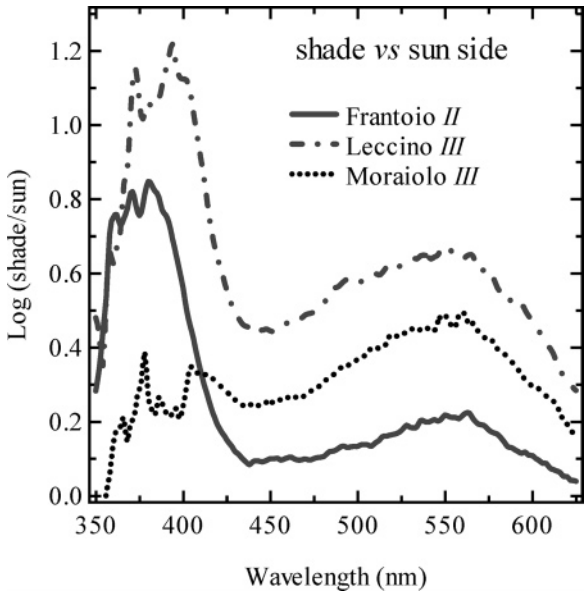

Figure 4. Absorbance spectra obtained from the logFER of sun-shaded vs sun-exposed olive surfaces. Measurements on three different olives of the Frantoio, Leccino, and Moraiolo cultivars are reported.

respect to the absorbance spectra measured in vivo (peak at 550 nm). The bathochromic shift observed in vivo may be explained as due to copigmentation (*35*) or to a vacuolar pH higher than that used in vitro (pH 2.0) (*36*, *37*). In particular, judging from a previous study on cyanidin-3-glycosides (*37*), the in vivo maximum recorded here at 550 nm would indicate a vacuolar pH between 6 and 7, in the absence of copigmentation. The green absorption band of the olive extract corresponds to that of cyanidin-3-O-rutinoside in the same solvent (see extinction coefficient spectrum in **Figure 3c**, dashed line). This compound was identified by HPLC analysis as the most abundant Anth present in olives (data not shown) in agreement with previous works (*17*, *18*).

Our results prove that the logFER spectral technique is suitable for revealing in vivo the absorption spectrum of pigments accumulated on the epidermal layers of olive fruits. As is common in several fruits, the olive samples showed well distinct differences between the sun-exposed and sun-shaded surfaces. The former appeared more protruded and red-colored with respect to their relative shaded side. On the other hand, it is well-known that Anth formation and accumulation are light intensity-dependent processes (*38*−*40*). We can thus apply our method to zones of different pigmentation on the same olive. The logFER calculated by ChlF excitation from the sun-exposed vs the sun-shaded sides (**Figure 4**) corresponds now to the difference in absorbance between the two olive surfaces. For all *O. europaea* cultivars studied, the sun-exposed olive side accumulated higher amounts of Anths than the shaded side in accordance with the light-driven biosynthesis of Anths (*40*). Similar conclusions were reached in apples by reflectance spectroscopy (*41*).

Assessment of Anth Content in Vivo. Comparing ChlF excitation of olives at different color stages, it is possible to nondestructively monitor the change in superficial pigments during fruit maturation (**Figure 5**). **Figure 5a**,**b** reports the absorbance spectra deduced from the logFER of olives at increasing stages of ripening (color levels II, III, and IV) vs green olive (color level I) for Frantoio (**a**) and Leccino (**b**) cultivars, respectively. They can be compared to the absorbance spectra measured in ethanol/water (pH 2.0) extracts of the very same olive zones used for the ChlF excitation measurements (**Figure 5c**,**d**). The logFER spectra showed well in vivo what can be observed in the difference absorbance spectra of the extracts. As expected, the Anth band increased with increasing maturation. Furthermore, the trend of the UVA-absorbing compounds in the logFER was similar to that in vitro for all combinations of logFER, both for Frantoio and Leccino, even though the UVA-absorbing compounds behaved differently in the two cultivars.

So, we have shown that the logFER spectral method is adequate for pigment identification in fruits at different maturation stages. Furthermore, it can be useful to define the best excitation wavelengths for the monitoring of specific compounds. Indeed, for absolute quantitative purposes, the two-wavelength logFER is more convenient. It compares the ChlF signal excited with light that is particularly well-absorbed and attenuated by the sampled pigment to that induced by light reaching Chl without attenuation. For Anths, we used the 550 nm light corresponding to their in vivo absorption maximum and a red light at 625 nm for the reference. The ChlF signal excited at 625 nm behaves like a kind of internal standard.

Figure 6 depicts the relationship between Anth absorbance assessed by the logFER method, using two excitation wavelengths, 625 and 550 nm, and emission at 740 nm, and the Anth concentration measured from olive extracts. All data from the three different cultivars were considered. The best fit was a power function (solid line in **Figure 6**) with a coefficient of determination $r^2 = 0.96$:

$$\log \frac{\mathrm{Chl}F^{740}(625)}{\mathrm{Chl}F^{740}(550)} = -0.475 + 0.677 \cdot (C_{\mathrm{Anth}})^{0.149} \quad (6)$$

where C_{Anth} is the Anth content per unit surface (nmol cm^{-2}).

It is worth noting that the logFER value for green Anth-free olives is not nil. This is probably due to the term $\log [(1-10^{-[\epsilon_a(625)c_a+\epsilon_b(625)c_b)l]}/(1-10^{-[\epsilon_a(550)c_a+\epsilon_b(550)c_b)l]}]$, defined in eq 5, because of a slight difference in the molar absorptivities of Chls at the two excitation wavelengths. In fact, this value calculated using the in vitro Chl a and b molar extinction coefficients (*27*) and the average Chls concentrations measured in green olives (10.6 and 5.8 μg cm^{-2}, for Chl a and b, respectively) was equal to 0.5, close to the lowest logFER values (0.4) recorded (cf. **Figure 6**).

The logFER vs Anths relationship can also be considered as linear for Anth concentrations up to about 70 nmol cm^{-2}; thereafter, a saturation effect occurs. In any case, the nonlinearity of the absorbances measured in vivo compared to those in vitro can have two types of origins: One is related to the inherent spectroscopic characteristics of Anths, and the other is related to the limits of the logFER method.

As already mentioned, the molar extinction coefficient and the position of the absorption maximum of Anths depend on the solvent and pH (*36*, *37*). Copigmentation (and self-association) not only affects both of these spectroscopic characteristics but can also be responsible for deviations from the Beer−Lambert's law associated with dilution (negative or positive depending on pH) (*36*). In addition, the extinction coefficient at the absorption maximum of Anths at pH 6 (in vivo) can be 3−9 times lower than that measured at pH 2 (in vitro) (*37*), in accordance with the ratio of the in vitro and the in vivo data presented in **Figure 3**. Finally, the acid hydrolysis of glycosidic bonds or acylation artifacts can also change the Anth characteristics after extraction. Still, the observed curvature (cf. **Figure 6**) can be even better explained by the limits of the logFER method itself.

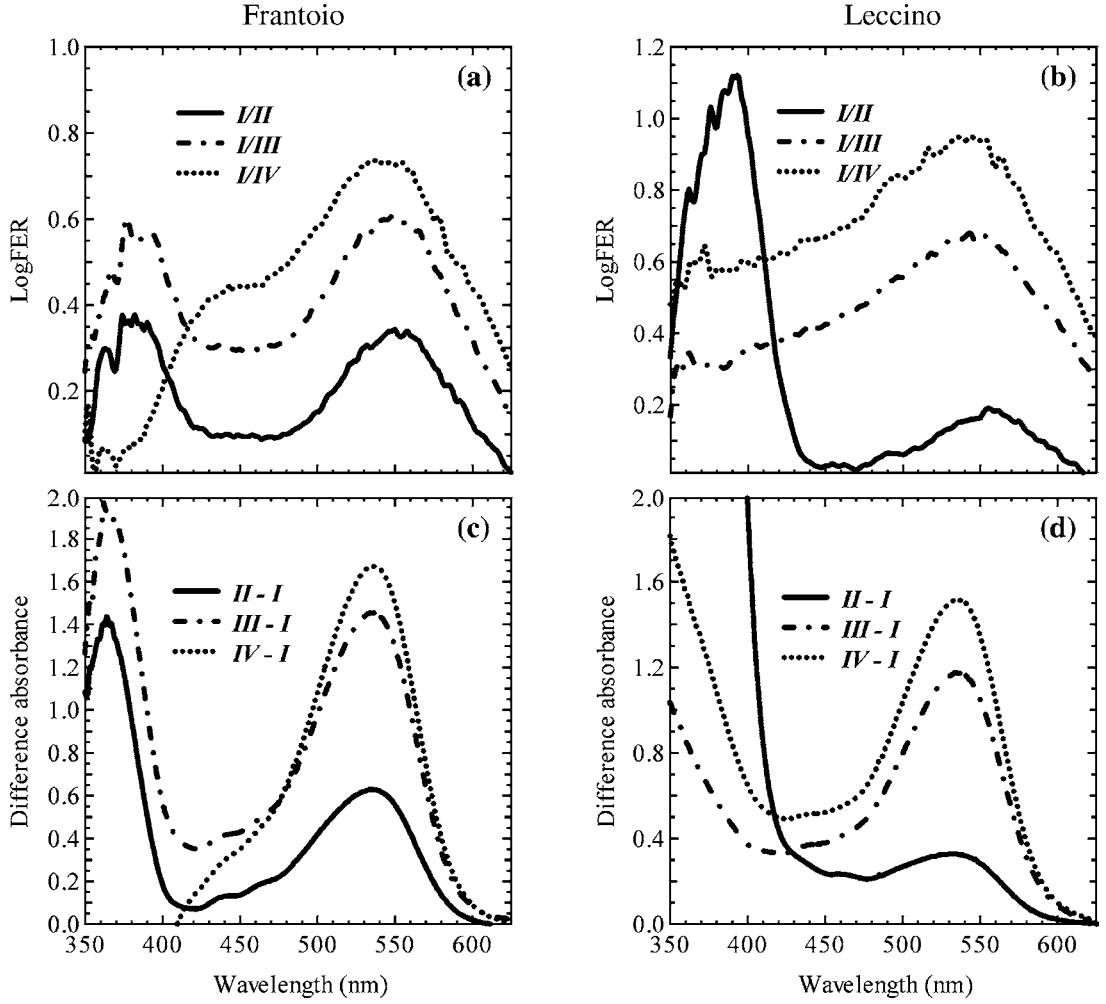

Figure 5. Absorbance spectra derived from the logFER of olives at increasing ripening stages vs green olive (color level I) for Frantoio (**a**) and Leccino (**b**) cultivars. Difference absorbance spectra of panels **c** and **d** are derived from ethanol/water (pH 2.0) extracts of the very same olive zones used for the ChlF excitation measurements of panels **a** and **b**, respectively.

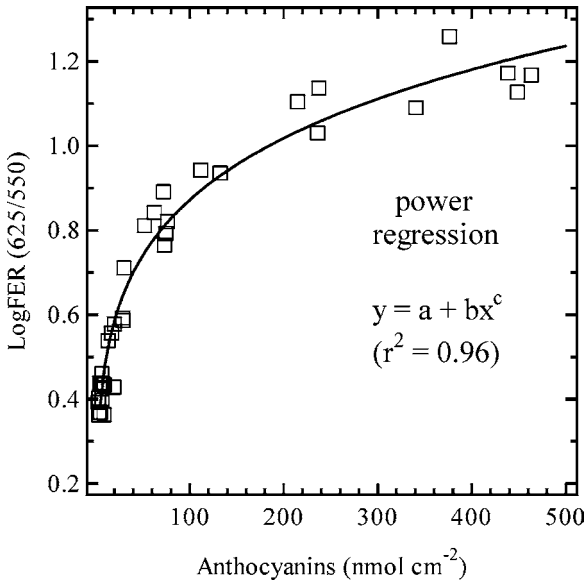

Figure 6. Relationship between Anth absorbance assessed nondestructively by the logFER at two excitation wavelengths, 625 and 550 nm, and the Anth concentration measured in the disk olive extracts. The emission wavelength was at 740 nm.

We have identified four effects that can be present individually or in combination when acquiring the logFER: (i) pigment vs fluorophore distribution, (ii) surface fluorescence, (iii) stray light, and (iv) sieve effect.

(i) As described in the Materials and Methods section and reported in the literature (*22*, *25*), the applicability of the logFER method is highest when the pigment-filtering layer is above the Chl region. When the absorber is not strictly confined to the upper layer (epidermis) above the fluorescing Chl but is present both in the epidermis and in the mesophyll of the leaf, or in the present study in the mesocarp of olive fruit, a curvature in the absorption against concentration graph (cf. **Figure 6**) can be induced if the proportion of the absorber is changing.

The pigment distribution inside the olive mesocarp can be observed in the microimage of **Figure 7a** that represents the RGB color recombination of monochrome transmittance images of a Frantoio olive cross-section (color level II) recorded in sequence at 450, 550, and 680 nm, for the blue, green, and red spectral bands, respectively. It clearly shows in red the Anth distribution within the first 200 μm from the surface. In **Figure 7b**, the localization of Chl is visualized by the fluorescence image at 680 nm, excited at 365 nm. An increase of Chl concentration is observed going from the epidermal layer to inside the mesocarp. The colocalization of Anths and Chl is well-denoted by the intensity profiles reported in **Figure 7c**. Here, the transmittance at 550 nm (T^{550}) that is inversely related to the Anth content and the ChlF (F^{680}) are plotted as a function of the depth. It can be seen that the two pigments are not

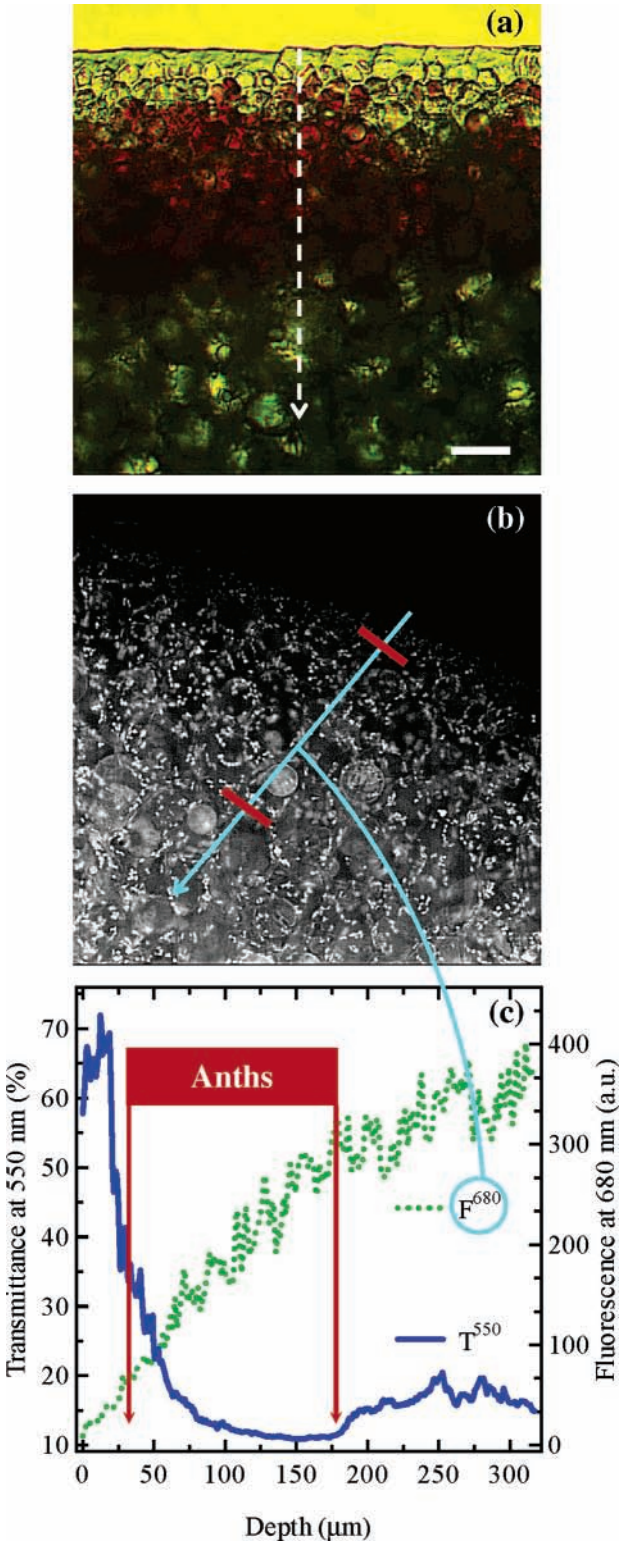

Figure 7. Microscopic analysis of a green–red olive cross-section (Frantoio cultivar). (**a**) RGB color recombination of three monochrome transmission images acquired in sequence at 450, 550, and 680 nm for the blue, green, and red bands, respectively; the bar corresponds to 50 μm. (**b**) Fluorescence image acquired at 680 nm for excitation at 365 nm; red segments indicate the tissue region where Anths accumulated. (**c**) Profiles of ChlF (F^{680}) and transmittance (T^{550}) from the peel into the olive mesocarp as mean intensity of each longitudinal row of pixels vs the depth; F^{680} was measured along the direction indicated by the arrow in panel **b**; T^{550} was measured on the transmitted image at 550 nm along the direction indicated by the white dashed arrow in panel **a**; the red area indicates the zone of Anth accumulation in the tissue.

spatially separated since Chl is present within the Anth region (red zones in **Figure 7**). This effect that is even expected to be more pronounced for mature olives where the Anth layer is thicker is probably the best candidate to explain the nonlinear behavior of the logFER vs Anths relationship reported in **Figure 6**.

(ii) Fluorescing structures, like Chl in the guard cell of leaf stomata or lenticelles in olive fruits, always contribute to the fluorescence signal independently of how much of the underlying Chl is screened by the absorber that we want to measure (here Anths). This contribution is negligible at low absorber contents (small screening) but becomes important at high absorbances (large screening), contributing, in the extreme case, to all of the fluorescence signal and bringing the absorption vs concentration graph to a saturation level.

(iii) Any measure of absorbance, and therefore the logFER method, has a limited range of operation defined by the presence of stray (unwanted) light in the spectrophotometer. The relative importance of stray light increases with absorbance (smaller transmittance of specific light), leading to a curvature of the measured absorbance and eventually limiting the maximum value of absorbances to 3 or 4 (0.1 and 0.01% transmittance, respectively) in an average spectrophotometer. Although based on fluorescence, the logFER method measures absorbance as a difference between two signals; therefore, it is also affected by the described phenomenon.

(iv) The incoming excitation light channeled into the sample through the cell walls is not affected by the screening absorbers, which are usually present in the vacuole. This is called the sieve effect and again puts a limit on the maximum possible absorbance measured by the logFER method.

According to eq 5, changes in both Chl a and b contents during maturation may also affect the logFER determination of Anths, by introducing a distortion factor. We observed that going from green (level I) to purple (level V) olives, Chl a and b decreased by 35 and 15%, respectively. However, this variation, because of the similarity of the Chl extinction coefficients at 550 and 625 nm, produced only a small effect (7% decrease in the distortion factor).

Relationship between Anths and Other Pigments. As previously demonstrated, Chl content can also be estimated by ChlF emission ratios detecting both the Chl emission maxima at 685 and 740 nm at two different excitation wavelengths (*21*). It is therefore possible using ChlF measurements to monitor at the same time both Anths and Chl. This prospect is particularly attractive for following the maturation process in fruits. In fact, often the accumulation of Anths is not correlated to a degradation of Chl or these changes may occur not simultaneously.

The relationship between Anths and other phenolic compounds present in the whole olive fruits was evaluated for the Frantoio cultivar and is shown in **Figure 8**.

As previously reported (*18*), four main classes of compounds were found as follows: (i) secoiridoids (oleuropein and its derivatives), (ii) low molecular weight phenolics (hydroxytyrosol and its glucoside), (iii) caffeic glycoside esters (verbascoside and hydroxyverbascoside), and (iv) flavonols (rutin and quercetin). These later (flavonols) occurred at low levels since their localization was limited to the peel as we observed by fluorescence microscopy of olive cross-sections (data not shown) and in agreement with previous works (*15*). They did not change significantly in relation to Anth content. Secoiridoids also presented small variations with Anths apart from the initial rapid decrease below a concentration of about 40 nmol cm^{-2}. Both

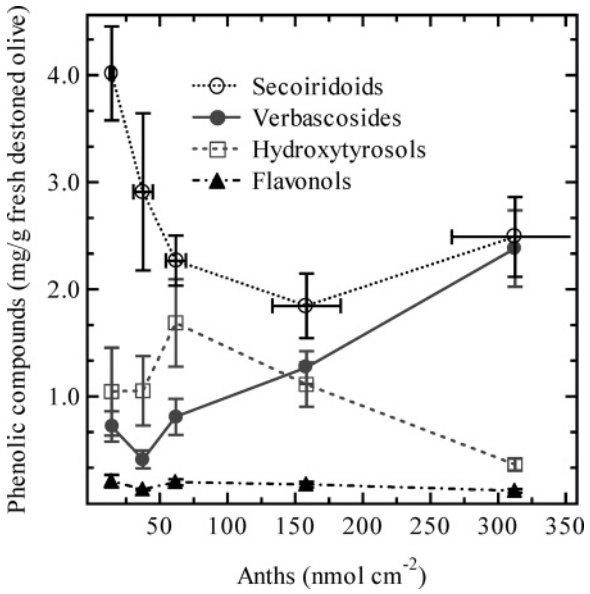

Figure 8. Relationship between phenolic compounds of destoned olives (mg per gr fresh weight) at different pigmentation and Anth surface concentration (nmol cm^{-2}). Data are means ± SD, $n = 3$. The SD for Anths is reported on the points of secoiridoids.

hydroxytyrosols and verbascosides showed a significant trend with Anth increase, decreasing and increasing, respectively.

To our knowledge, this is the first study aimed at quantitatively relating the Anth content to that of other phenolics in olives. Comparison with previous works on the phenolic profile and content related to fruit maturation is difficult. In fact, the evolution of the main compounds with olive ripening has been reported as a function of the harvesting time with reference to skin color data such as appearance, maturation indexes, and colorimetric parameters but not Anth content. The occurrence of rapid fluctuations in specific phenolics, as observed with sequential sampling dates, and the effect of alternate fruit bearing (*16*) may also complicate data interpretation. Taking this into account, we can note that the increase in verbascoside with Anth content agrees with the verbascoside augmentation during olive ripening previously observed (*13*, *15*, *16*). Because verbascoside is a disaccharide linked to hydroxytyrosol and caffeic acid moieties formed by glucoside conjugation of hydroxytyrosol and caffeic acid, it is reasonable to expect that variations of these compounds be related to each other. Indeed, as the verbascoside amount tripled going from green to purple olives, hydroxytyrosol was reduced to one-third. We did not obtain accurate data for caffeic acid because it occurred at very low levels; however, its trend with Anths was similar to that of hydroxytyrosol (data not shown). Caffeic acid can also actively take part in the acylation of Anths; however, we did not observe significant amounts of acylated compounds suggesting that caffeic acid remained sequestered in the verbascoside molecules.

Verbascoside evaluation in olive fruits can be of interest from a pharmacological point of view. In fact, verbascoside, having two catecholic moieties in its structure, has peculiar antioxidant properties. In particular, verbascoside protects the cell from oxidative stress and its scavenging of free radicals could be a key mechanism contributing to a cytoprotective effect (*42*, *43*). Oxidative stress is also regarded to be a major etiologic factor for many cancers and heart diseases; hence, verbascoside could be an important modulator of cancer chemopreventive activity (*44*, *45*) and could inhibit some macrophage functions involved in the inflammatory process (*46*).

The observed relationship between Anths and verbascoside indicates that accumulation of the caffeic glycoside ester in the pulp can be indirectly monitored by the optical noninvasive evaluation of Anths on the surface. This possibility, once confirmed for other cultivars, could be of real interest to develop agronomic methods that maximize verbascoside accumulation in olive fruits. Because this valuable compound could be recovered from the olive mill wastewaters (*6*), knowing its drupe concentration at harvest may help in predicting the recovery efficiency and convenience.

In conclusion, ChlF techniques have previously been indicated as tools to assess fruit quality (*47*). They are mainly based on the evaluation of the fruit photosynthetic activity by measuring typical parameters of the ChlF variation occurring during the dark to light transition (Kautsky effect). These methods require a dark adaptation of the samples limiting their practical usefulness especially for in field applications. The FER approach that we have adopted for this study is still based on ChlF but provides nondestructive quantitative data on the pigments in the superficial layers of the fruit. In particular, it is possible to estimate the amount of Anths that are directly related to fruit maturity.

Recently, another noninvasive optical technique based on diffuse reflectance spectroscopy was suggested for Anths assessment in apples (*41*, *48*). The value of reflectance spectroscopy with respect to the FER method can be estimated only through a direct comparison between them. However, several advantages in the logFER method can be envisaged. First of all, in reflectance spectroscopy, the Chl and carotenoid absorption bands overlap the Anth band reducing the specificity of Anth determination. This effect is not present in the Anth absorbance deduced by the logFER method. Moreover, as the logFER is based on the ratio of fluorescence at two excitation wavelengths, it is independent of the shape and size of the samples. In reflectance spectroscopy, the fact that the signal depends on the angle between illumination and detection may be a problem for the measurement of small samples such as olives. Finally, the logFER method can provide information on flavonoids and hydroxycinnamates absorbing in the UV, while in this spectral range reflectance is very low and difficult to be measured.

According to our results, new portable optoelectronic devices for the nondestructive monitoring of olive development and ripening can be developed. They can provide automatic maturation indexes directly related to pigment concentrations and, therefore, are expected to be more reliable than those merely based on the subjective visual classification through olive skin colors (*7*). A LogFER-based ripening index should also be better than colorimetric procedures (*8*), which use broad bandwidth reflectance signals. It can solve the problem of carefully defining the olive maturation stages that is fundamental for comparing the ripening-related features observed in different studies.

ABBREVIATIONS USED

Anth(s), anthocyanin(s); CCD, charge-coupled device; Chl, chlorophyll; ChlF, chlorophyll fluorescence; FER, fluorescence excitation ratio; logFER, logarithm of the FER; QSEU, quinine sulfate equivalent units; RGB, red green blue.

ACKNOWLEDGMENT

Z.G.C. and A.C. thank Nicolae Moise, Yves Goulas, Abderrahmane Ounis, and Sylvie Meyer for support and assistance.

LITERATURE CITED

(1) Zohary, D.; Spiegel-Roy, P. Beginning of fruit growing in the Old World. *Science* **1975**, *187*, 319−327.

(2) Liphschitz, N.; Gophna, R.; Hartnan, M.; Biger, G. The beginning of olive (*Olea europaea* L.). Cultivation in the old word: A reassessment. *J. Archaeol. Sci.* **1991**, *18*, 441−453.

(3) Baldioli, M.; Servili, M.; Peretti, G.; Montedoro, G. F. Antioxidant activity of tocopherols and phenolic compounds of virgin olive oil. *J. Am. Oil Chem. Soc.* **1996**, *73*, 1589−1593.

(4) Servili, M.; Montedoro, G. Contribution of phenolic compounds to virgin olive oil quality. *Eur. J. Lipid Sci. Technol.* **2002**, *104*, 602−613.

(5) Visioli, F.; Galli, C. Oleuropein protects low-density lipoprotein from oxidation. *Life Sci.* **1994**, *55*, 1965−1971.

(6) Mulinacci, N.; Romani, A.; Pinelli, P.; Galardi, C.; Giaccherini, K.; Vincieri, F. F. Polyphenolic content in olive oil wastewaters and related olive samples. *J. Agric. Food Chem.* **2001**, *49*, 3509−3514.

(7) IOOC. *Document No. 6*; International Olive Oil Council: Madrid, 1984.

(8) Esti, M.; Cinquanta, L.; La Notte, E. Phenolic compounds in different olive varieties. *J. Agric. Food Chem.* **1998**, *46*, 32−35.

(9) Ryan, D.; Antolovich, M.; Prenzler, P. D.; Robards, K.; Lavee, S. Biotransformations of phenolic compounds in *Olea europaea* L. *Sci. Hortic.* **2002**, *92*, 147−176.

(10) Minguez-Mosquera, I.; Gallardo-Guerrero, L. Disappearance of chlorophylls and carotenoids during the ripening of the olive. *J. Sci. Food Agric.* **1995**, *69*, 1−6.

(11) Abbott, J. A. Quality measurements of fruits and vegetables. *Postharvest Biol. Technol.* **1999**, *15*, 207−225.

(12) Jaakola, L.; Maatta, K.; Pirttila, A. M.; Torronen, R.; Karenlampi, S.; Hohtola, A. Expression of genes involved in anthocyanin biosynthesis in relation to anthocyanin, proanthocyanidin, and flavonol levels during bilberry fruit development. *Plant Physiol.* **2002**, *130*, 729−739.

(13) Amiot, M. J.; Fleuriet, A.; Macheix, J. J. Importance and evolution of phenolic compounds in olive during growth and maturation. *J. Agric. Food Chem.* **1986**, *34*, 823−826.

(14) Briante, R.; Patumi, M.; Limongelli, S.; Febbraio, F.; Vaccaro, C.; Di Salle, A.; La Cara, F.; Nucci, R. Changes in phenolic and enzymatic activities content during fruit ripening in two Italian cultivars of *Olea europaea* L. *Plant Sci.* **2002**, *162*, 791−798.

(15) Servili, M.; Baldioli, M.; Selvaggini, R.; Macchioni, A.; Montedoro, G. Phenolic compounds of olive fruit: One- and two-dimensional nuclear magnetic resonance characterization of Nuzhenide and its distribution in the constitutive parts of fruit. *J. Agric. Food Chem.* **1999**, *47*, 12−18.

(16) Ryan, D.; Prenzler, P. D.; Lavee, S.; Antolovich, M.; Robards, K. Quantitative changes in phenolic content during physiological development of the olive (*Olea europaea*) cultivar Hardy's Mammoth. *J. Agric. Food Chem.* **2003**, *51*, 2532−2538.

(17) Vlahov, G. Flavonoids in three olive (*Olea europaea*) fruit varieties during maturation. *J. Sci. Food Agric.* **1992**, *58*, 157−159.

(18) Romani, A.; Mulinacci, N.; Pinelli, P.; Vincieri, F. F.; Cimato, A. Polyphenolic content in five Tuscany cultivars of *Olea europaea* L. *J. Agric. Food Chem.* **1999**, *47*, 964−967.

(19) Romero, C.; Garcia, P.; Brenes, M.; Garcia, A.; Garrido, A. Phenolic compounds in natural black spanish olive varieties. *Eur. Food Res. Technol.* **2002**, *215*, 489−496.

(20) Bilger, W.; Veit, M.; Schreiber, L.; Schreiber, U. Measurement of leaf epidermal transmittance of UV radiation by chlorophyll fluorescence. *Physiol. Plant* **1997**, *101*, 754−763.

(21) Ounis, A.; Cerovic, Z. G.; Moya, I.; Briantais, J. M. Dual-excitation FLIDAR for the estimation of epidermal UV absorption in leaves and canopies. *Remote Sens. Environ.* **2001**, *76*, 33−48.

(22) Cerovic, Z. G.; Ounis, A.; Cartelat, A.; Latouche, G.; Goulas, Y.; Meyer, S.; Moya, I. The use of chlorophyll fluorescence excitation spectra for the nondestructive in situ assessment of UV-absorbing compounds in leaves. *Plant Cell Environ.* **2002**, *25*, 1663−1676.

(23) Goulas, Y.; Cerovic, Z. G.; Cartelat, A.; Moya, I. DUALEX: A new instrument for field measurements of epidermal UV absorbance by chlorophyll fluorescence. *Appl. Opt.* **2004**, *43*, 4488−4496.

(24) Cartelat, A.; Cerovic, Z. G.; Goulas, Y.; Meyer, S.; Lelarge, C.; Prioul, J. L.; Barbottin, A.; Jeuffroy, M.-H.; Gate, P.; Agati, G.; Moya, I. Optically assessed polyphenolics and chlorophyll content of leaves as indicators of nitrogen deficiency in wheat. *Field Crops Res.* **2005**, *91*, 35−49.

(25) Bilger, W.; Johnsen, T.; Schreiber, U. UV-excited chlorophyll fluorescence as a tool for the assessment of UV-protection by the epidermis of plants. *J. Exp. Bot.* **2001**, *52*, 2007−2017.

(26) Kolb, C. A.; Kopecky, J.; Riederer, M.; Pfundel, E. E. UV screening by phenolics in berries of grapevine (*Vitis vinifera*). *Funct. Plant Biol.* **2003**, *30*, 1177−1186.

(27) Cerovic, Z. G.; Samson, G.; Morales, F.; Tremblay, N.; Moya, I. Ultraviolet-induced fluorescence for plant monitoring: Present state and prospects. *Agronomie* **1999**, *19*, 543−578.

(28) Agati, G.; Galardi, C.; Gravano, E.; Romani, A.; Tattini, M. Flavonoid distribution in tissues of *Phillyrea latifolia* L. leaves as estimated by microspectrofluorometry and multispectral fluorescence microimaging. *Photochem. Photobiol.* **2002**, *76*, 350−360.

(29) Gould, K. S.; Markham, K. R.; Smith, R. H.; Goris, J. J. Functional role of anthocyanins in the leaves of *Quintinia serrata* A. Cunn. *J. Exp. Bot.* **2000**, *51*, 1107−1115.

(30) Lichtenthaler, H. Chlorophylls and carotenoids: Pigments of photosynthetic biomembranes. *Methods Enzymol.* **1987**, *148*, 350−382.

(31) Baldi, A.; Romani, A.; Mulinacci, N.; Vincieri, F. F.; Casetta, B. HPLC/MS application to anthocyanins of *Vitis vinifera* L. *J. Agric. Food Chem.* **1995**, *43*, 2104−2109.

(32) Mulinacci, N.; Innocenti, M.; Giaccherini, C.; Romani, A.; Vincieri, F. F.; Morazzoni, P.; Riva, A.; Mercalli, E. Chemical characterisation of verbascoside analogues from solid olive residues of cv. Coratina. In *Polyphenols Communications 2002*; El Hadrami, I., Ed.; El Watanya: Marrakech, 2002; pp 567−568.

(33) Rabinowitch, E. I. *Photosynthesis and Related Processes*; Interscience: New York, 1951.

(34) Lichtenthaler, H. K.; Buschmann, C.; Rinderle, U.; Schmuck, G. Application of chlorophyll fluorescence in ecophysiology. *Radiat. Environ. Biophys.* **1986**, *25*, 297−308.

(35) Boulton, R. The copigmentation of anthocyanins and its role in the color of red wine: A critical review. *Am. J. Enol. Vitic.* **2001**, *52*, 67−87.

(36) Strack, D.; Wray, V. Anthocyanins. In *Methods in Plant Biochemistry—Plant Phenolics*; Dey, P. M., Harborne, J. B., Eds.; Academic Press: London, 1989; pp 325−356.

(37) Fossen, T.; Cabrita, L.; Andersen, Ø. M. Colour and stability of pure anthocyanins influenced by pH including the alkaline region. *Food Chem.* **1998**, *63*, 435−440.

(38) Saure, M. C. External control of anthocyanin formation in apple. *Sci. Hortic.* **1990**, *42*, 181−218.

(39) Mancinelli, A. L.; Rossi, F.; Moroni, A. Cryptochrome, phytochrome, and anthocyanin production. *Plant Physiol.* **1991**, *96*, 1079−1085.

(40) Chalker-Scott, L. Environmental significance of anthocyanins in plant stress responses. *Photochem. Photobiol.* **1999**, *70*, 1−9.

(41) Merzlyak, M. N.; Chivkunova, O. B. Light-stress-induced pigment changes and evidence for anthocyanin photoprotecion in apples. *J. Photochem. Photobiol., B* **2000**, *55*, 155−163.

(42) Chiou, W. F.; Lin, L. C.; Chen, C. F. Acteoside protects endothelial cells against free radical-induced oxidative stress. *J. Pharm. Pharmacol.* **2004**, *56*, 743−748.

(43) Lee, K. J.; Woo, E. R.; Choi, C. Y.; Shin, D. W.; Lee, D. G.; You, H. J.; Jeong, H. G. Protective effect of acteoside on carbon tetrachloride-induced hepatotoxicity. *Life Sci.* **2004**, *74*, 1051−1064.

(44) Pettit, G. R.; Numata, A.; Takemura, T.; Ode, R. H.; Narula, A. S.; Schmidt, J. M.; Cragg, G. M.; Pase, C. P. Antineoplastic agents, 107. Isolation of acteoside and isoacteoside from *Castilleja linariaefolia*. *J. Nat. Prod.* **1990**, *53*, 456−458.

(45) Owen, R. W.; Haubner, R.; Mier, W.; Giacosa, A.; Hull, W. E.; Spiegelhalder, B.; Bartsch, H. Isolation, structure elucidation and antioxidant potential of the major phenolic and flavonoid compounds in brined olive drupes. *Food Chem. Toxicol.* **2003**, *41*, 703−717.

(46) Diaz, A. M.; Abad, M. J.; Fernandez, L.; Silvan, A. M.; De Santos, J.; Bermejo, P. Phenylpropanoid glycosides from *Scrophularia scorodonia*: In vitro antiinflammatory activity. *Life Sci.* **2004**, *74*, 2515−2526.

(47) DeEll, J. R.; van Kooten, O.; Prange, R. K.; Murr, D. P. *Applications of Chlorophyll Fluorescence Techniques in Postharvest Physiology*; Janick, J., Ed.; John Wiley & Sons: New York, 1999.

(48) Merzlyak, M. N.; Solovchenko, A. E.; Gitelson, A. A. Reflectance spectral features and nondestructive estimation of chlorophyll, carotenoid and anthocyanin content in apple fruit. *Postharvest Biol. Technol.* **2003**, *27*, 197−211.

Received for review September 28, 2004. Revised manuscript received December 21, 2004. Accepted December 23, 2004. This work was supported by the CNR (Italy)−CNRS (France) bilateral cooperation Project 11409.

JF048381D